

## INFLUENCE OF MICROSTRUCTURE ON SULPHIDE STRESS CRACKING OF HOT ROLLED TUBES

Sojka J.<sup>1</sup>, Jonšta P.<sup>1</sup>, Rytířová L.<sup>1</sup>, Sozańska M.<sup>2</sup>, Jérôme M.<sup>3</sup>

<sup>1</sup>VŠB – Technical University of Ostrava, Faculty of Metallurgy and Materials Engineering, 17. listopadu 15, 708 33 Ostrava-Poruba, Czech Republic

<sup>2</sup>Silesian University of Technology, Krasińskiego 8, Katowice, Poland

<sup>3</sup>Ecole Centrale Paris, Grande Voie des Vignes, 92295 Châtenay-Malabry CEDEX, France  
E-mail: jaroslav.sojka@vsb.cz; mariasoz@mail.polsl.katowice.pl; michel.jerome@ecp.fr

## VLIV MIKROSTRUKTURY NA SULFIDICKÉ PRASKÁNÍ POD NAPĚTÍM ZA TEPLA VÁLCOVANÝCH TRUBEK

Sojka J.<sup>1</sup>, Jonšta P.<sup>1</sup>, Rytířová L.<sup>1</sup>, Sozańska M.<sup>2</sup>, Jérôme M.<sup>3</sup>

<sup>1</sup>VŠB – Technická univerzita Ostrava, Fakulta metalurgie a materiálového inženýrství, 17. listopadu 15, 708 33 Ostrava-Poruba, Česká republika

<sup>2</sup>Politechnika Śląska, Krasińskiego 8, Katowice, Polsko

<sup>3</sup>Ecole Centrale Paris, Grande Voie des Vignes, 92295 Châtenay-Malabry CEDEX, Francie  
E-mail: jaroslav.sojka@vsb.cz; mariasoz@mail.polsl.katowice.pl; michel.jerome@ecp.fr

### Abstrakt

Předložený příspěvek shrnuje výsledky hodnocení odolnosti za tepla válcovaných trub vůči sulfidickému praskání pod napětím. Dvě oceli, X52 a X60, které byly vyrobeny v souladu s předpisem API 5L, byly testovány jednak ve výchozím stavu (po válcování za tepla), jednak po laboratorním zušlechtnění, které sestávalo z kalení do vody z kalicí teploty 870°C a následného vysokoteplotního popouštění při teplotě 600°C po dobu dvou hodin. Získané výsledky ukázaly, že odolnost ocelí vůči sulfidickému praskání pod napětím závisí velice významně na jejich mikrostruktuře, podobně jako tomu je v případě vodíkem indukovaného praskání. Odolnost vůči sulfidickému praskání pod napětím byla testována v souladu s předpisem NACE TM 0177. Oceli, které obsahovaly výrazné řádky perlitu nebo dokonce řádky nepopuštěného martenzitu a bainitu, vykazovaly nízkou odolnost vůči sulfidickému praskání pod napětím. Zušlechtnění mělo velmi příznivý vliv na odolnost vůči sulfidickému praskání přesto, že jejich pevnost a tvrdost vzrostly. Po zušlechtnění vzrostlo kritické napětí pro sulfidické praskání pod napětím o 180 až 200 MPa. Významné rozdíly byly zjištěny i v hodnotách koeficientu difuze vodíku pro rozdílné stavy. Koeficient difuze vodíku byl stanoven metodou elektrochemické permeace vodíku na vzorcích charakteru tenkých membrán. Po zušlechtnění byl koeficient difuze vodíku výrazně nižší. Všechny získané výsledky ukazují, že mikrostruktura je velmi důležitým činitelem při hodnocení odolnosti ocelí vůči sulfidickému praskání pod napětím. Nerespektování této skutečnosti může znamenat použití neodolných ocelí se všemi negativními důsledky.

### Abstract

Presented paper summarizes results of sulphide stress cracking resistance of hot rolled tubes made of carbon steels. Two grades of steels - X52 and X60, that were manufactured according to API 5L Specification - have been tested in as-received state (after hot rolling) and

after laboratory quenching from 870°C temperature into water and subsequent tempering at 600°C for 2 hours. Obtained results have shown that sulphide stress cracking resistance of steels depends strongly on their microstructure as in the case of hydrogen induced cracking. Heats containing bands of ferrite and pearlite or even bands of non-tempered bainite or martensite exhibited a poor resistance to sulphide stress cracking and failed at stresses well below the yield point when tested according to NACE TM 0177, Method A. Quenching and tempering had a beneficial effect on sulphide stress cracking resistance despite the fact that mechanical properties and hardness increased considerably. The critical stress for sulphide stress cracking increased about 180 - 200 MPa after quenching and tempering. Differences have also been found in values of hydrogen diffusion coefficient for different structures. This coefficient was evaluated by means of electrochemical hydrogen permeation on thin membranes prepared of studied steels. The hydrogen diffusion coefficient was significantly lower for quenched and tempered state. All the results indicate that microstructure plays an important role in the case of sulphide stress cracking. If this fact is not respected, materials non-resistant to sulphide stress cracking can be chosen.

**Keywords:** Sulphide stress cracking, carbon steel, segregation bands, hydrogen permeation.

## 1. Introduction

Petroleum and natural gas systems can be contaminated with aqueous H<sub>2</sub>S. This environment is very aggressive to the steels used in the transport and processing of these products. The reaction between wet H<sub>2</sub>S and the steel generates atomic hydrogen, which can be, at least partially, absorbed into the steel. In the absence of applied stress, the diffused hydrogen can cause hydrogen induced cracking (HIC). The resistance of steels to HIC is closely related to the microstructure features: non-metallic inclusions, hard phase constituents, banded structures etc. [1-3]. In the presence of applied or residual stress, the failure process can occur by sulphide stress cracking (SSC) or stress oriented hydrogen induced cracking (SOHIC). In the case of SSC, steel resistance is commonly derived from its strength level. It is generally accepted that steels having tensile strength less than 690 MPa approx. are resistant to SSC [4,5]. The role of microstructure is not taken into the consideration although there are some works showing that microstructure can play an important role also in the case of SSC [6,7]. The presented paper evaluates the effect of microstructure (heat treatment) on the resistance of hot rolled tubes made from API X52 and X60 steels to SSC. To obtain detailed information about material behaviour in the presence of hydrogen, electrochemical permeation tests were performed as well.

## 2. Experimental procedure

The materials used in this study were tubes made of X52 (255/20 mm) and X60 (500/12 mm) steels meeting requirements of API 5L standard. Chemical composition of the studied steels is given in Table 1.

Table 1 Chemical composition of the steels (mass %)

Steel	C	Mn	Si	P	S	Cr	Ni	V	Nb	Ti
X52	0.09	0.92	0.28	0.007	0.01	0.02	0.01	0.004	0.03	0.01
X60	0.21	1.52	0.19	0.012	0.003	0.16	0.15	0.05	0.03	0.01

Steels were studied in two different states:

- in as-received state (AR) - after hot rolling;
- after laboratory quenching and tempering (QT) - 870°C/40 min/water + 600°C/2 hours/air.

For the laboratory heat treatment, testing coupons with dimensions 300 x 200 x thickness (mm) were used.

Structure analysis was performed by means of optical metallography (OM) and scanning electron microscopy (SEM). Tensile properties were determined using MTS 100 kN machine on cylindrical specimens with 10 mm in diameter and 50 mm in gauge length, taken from the mid-thickness of the materials. Notch toughness was measured on standard Charpy impact specimens at 0 °C.

Sulphide stress cracking was evaluated as required in NACE TM 0177 Standard, Method A. Subsize cylindrical specimens were used with diameter of 3.81 mm and gauge length of 25.4 mm. The applied load varied from 0.5 to 0.9 of the yield strength (YS) of the tested materials. Based on the test results, a critical stress could be evaluated for each of the tested steels and state.

Fracture surfaces of SSC test specimens were observed carefully using SEM. Prior to the observation, they were cleaned ultrasonically in a mild solution of H<sub>3</sub>PO<sub>4</sub> for 1 to 3 minutes.

Electrochemical permeation tests were derived from the Devanathan and Stachurski method [8]. They were performed at ambient temperature in a permeation cell composed of two double wall glass compartments separated by the sample (working electrode). Only X52 steel was tested in both AR and QT states. At entry side, a 0.05 M H<sub>2</sub>SO<sub>4</sub> solution was used. The exit side, previously coated with a thin layer of Pd [9], was polarised in 0.1 M NaOH solution at a constant potential of 0.28 V<sub>NHE</sub>. The anodic current recorded at the exit side was a measure of the permeation rate of hydrogen. Continuous argon bubbling was maintained during the whole test in both compartments. The membrane thickness was about 0.4 mm and its working area was 1.0 cm<sup>2</sup>.

After residual current density stabilisation, a first permeation was performed using a current density of -5 mA.cm<sup>-2</sup>. When the permeation rate achieved a steady-state level, the entry side was polarised anodically with a current density of 10 mA.cm<sup>-2</sup> to refresh the membrane surface. At the end of this period, charging solution (0.05 M H<sub>2</sub>SO<sub>4</sub>) was continuously renewed to eliminate metallic ions and three successive build-up transients were recorded using current densities of -5, -10 and -20 mA.cm<sup>-2</sup>. The diffusion coefficient of hydrogen was calculated from the beginning of permeation transients.

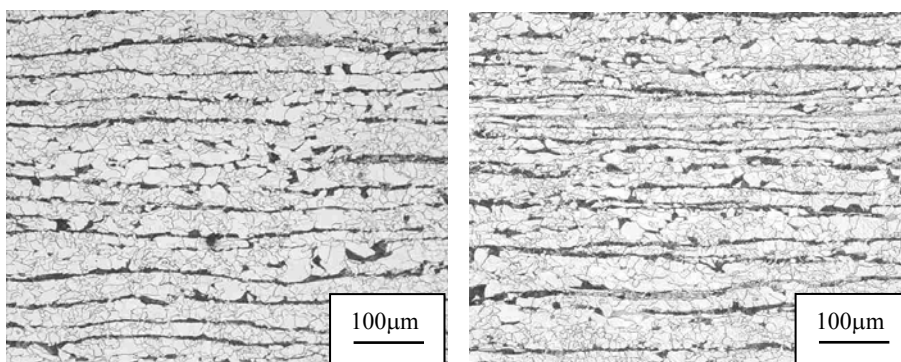
### 3. Results and discussion

#### 3.1 Microstructure

Examples of microstructure in as-received state are shown in Fig. 1a,b, respectively. For X52 steel, microstructure consisted predominantly of ferrite with some portion of pearlite, presented in the form of more or less pronounced bands. Non-tempered martensite was observed in some portions of these bands. In X60 API steel, microstructure contained ferrite, some amount of pearlite, but a rather high content of non-tempered martensite (Fig. 1b). The presence of martensite may be the result of a low tube thickness.

Laboratory quenching and tempering did not result in a fully martensitic or bainitic structure in the mid-thickness of X52 API steel. The microstructure corresponded rather to the

tempered bainite with some amount of ferrite. For X60 API steel, no ferrite was observed even in the mid-thickness and the microstructure was fully a tempered martensite. Banded structure, presented in as-received state, disappeared for both studied steels. Fig. 2a,b represent examples of steel microstructure after laboratory quenching and tempering.



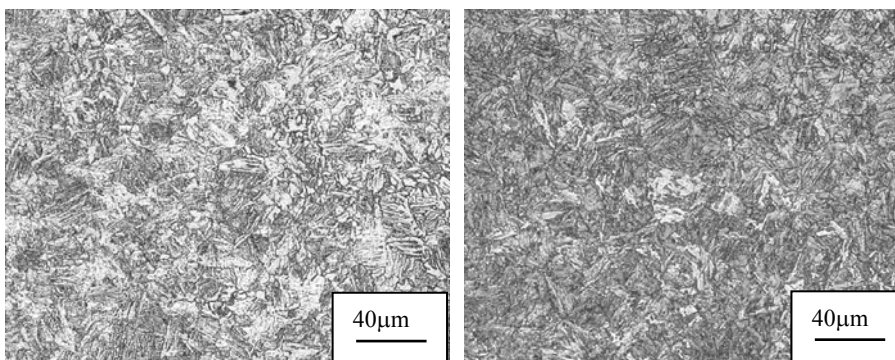
a) Ferrite and pearlite in X52 steel

b) Ferrite, pearlite and martensite in X60 steel

Fig.1 Microstructure in the mid-thickness of the steels in as-received state

### 3.2 Mechanical properties

Mechanical properties of the studied steels are summarised in Table 2. It is obvious that both steels meet standard requirements. Quenching and tempering considerably increased yield strength  $R_e$  and tensile strength  $R_m$  without any particular loss of plastic properties (elongation) and notch toughness. For X52 steel, the difference between yield strength in as-received and quenched and tempered state was about 100 MPa, for X60 API steel it was 140 MPa.



a) Tempered bainite and some ferrite in X52 API steel

b) Fully martensitic structure in X60 API steel.

Fig.2 Microstructure in the mid-thickness of the steels after laboratory quenching and tempering

Table 2 Mechanical properties of the studied steels

Steel	$R_e$ (MPa)	$R_m$ (MPa)	$A_5$ (%)	$KV_{0°C}$ (J)
X52/AR	390	515	24.5	196
X52/QT	486	610	22.6	218
X60/AR	593	770	21.8	148
X60/QT	733	792	20.2	165

### 3.3 Sulphide stress cracking tests

The results of SSC tests are summarised in the graphical form in Fig. 3.

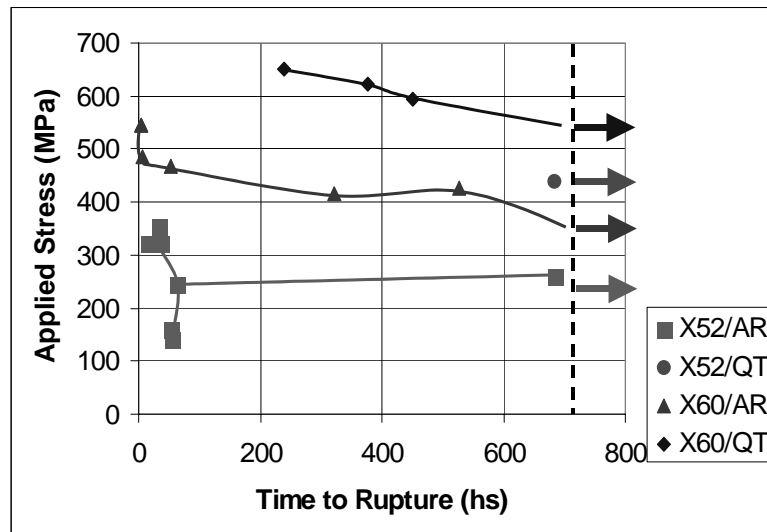


Fig.3 Results of SSC tests – Time to rupture as a function of the applied stress for the studied steels

In SSC the main role is generally attributed to the steel strength level and to its hardness [4,5]. The role of microstructure is not emphasised. Rules concerning the choice of SSC resistant materials presented in [5] are based on this approach. Nevertheless, heat treatment is mentioned in that document and in this way microstructure is, at least indirectly, taken into consideration. The presented results of SSC tests show clearly the same evolution as in the case of HIC testing [3,7] and confirm thus an important role of the microstructure in SSC process. Laboratory quenching and tempering, resulting in tempered martensitic structure or in a mixture of tempered bainite and ferrite, increased considerably steel resistance to SSC. A very similar behaviour was found in [6,7].

Indeed, X52 API steel withstood only a stress corresponding to 58% of the YS in as-received state. After the laboratory quenching and tempering the critical stress corresponded to 92% of the YS, being 486 MPa, as the YS also increased after QT. The absolute value of the difference between critical stresses in AR and QT states was more than 200 MPa! The behaviour was similar for X60 API steel. This steel withstood a stress corresponding to 60% of its YS in as-received state, i.e. about 356 MPa. After quenching and tempering the steel sustained a stress of 73% of the YS, i. e. about 535 MPa. In this case, the absolute value of the critical stress difference was still about 180 MPa, an important one.

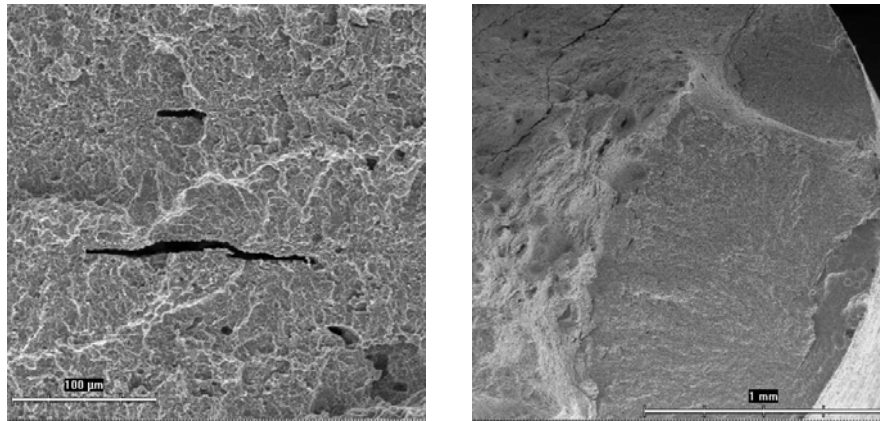
Examples of fracture surfaces of broken SSC specimens are shown in Fig. 4 for AR and QT states, respectively. Fracture surfaces consisted predominantly of quasicleavage fracture (QCF) with some larger cracks perpendicular to the fracture surface in as-received state. A rupture probably occurred as a sequence of HIC and SSC. Similar findings were presented in [7]. Despite the fact that large cracks were parallel to the loading direction they contributed to a rapid degradation and a short failure times in as-received state. In some smaller quasicleavage regions, which were circular or elliptical, some “holes” were observed in their centres. These

holes could correspond to the presence of non-metallic inclusions in steels, acting as SSC initiation sites. Nevertheless, no inclusions were identified there. It is possible that inclusions released from their sites during specimen ultrasonic cleaning prior to the SEM observation. Only a small portion of fracture surface corresponded to a transgranular ductile fracture

After laboratory quenching and tempering, fracture surfaces of broken SSC specimens were still predominantly quasicleavage, with some large regions of QCF and numerous small ones. The small regions resembled to those found in as-received state having “holes” in their centres. Even after quenching and tempering, no non-metallic inclusions were found there. In contrast to as-received state, no large cracks perpendicular to fracture surface were observed after quenching and tempering. It can be assumed there was not an important contribution of HIC during SSC tests after quenching and tempering.

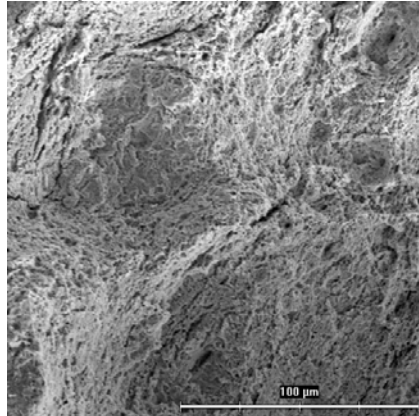
### 3.4 Electrochemical permeation tests

Tests were performed on X52 specimens, in AR and QT states. The direction of hydrogen diffusion was parallel to the pearlite bands of AR state. An example of permeation curves obtained during electrochemical permeation test is shown in Fig. 5 for AR state. Similar curves were obtained for QT state.



a) Fracture surface – X60 API steel/QT

b) Fracture surface – X60 API steel/QT



c) Quasicleavage areas with “holes” in their centres – X60 API steel/AR state

Fig.4 Fracture surfaces of SSC specimens

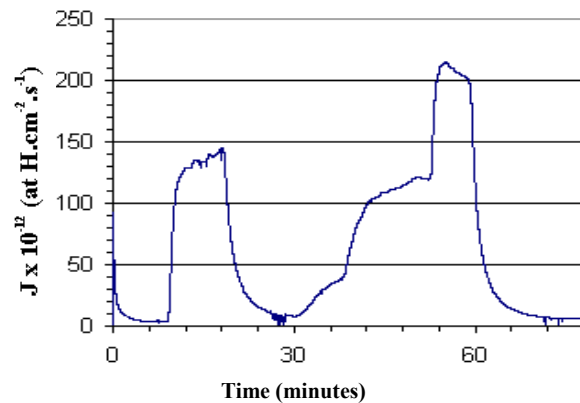


Fig.5 An example of permeation curves for X52 steel in as-received state

Hydrogen permeation currents were similar for both states. Apparent diffusion coefficients of hydrogen computed from permeation curves (first transient at  $-5 \text{ mA.cm}^{-2}$  after anodic attack and entry surface refreshment) were  $9.5.10^{-6} \text{ cm}^2.\text{s}^{-1}$  for X52 steel in AR state and only  $3.8.10^{-6} \text{ cm}^2.\text{s}^{-1}$  in QT state, the value being 2.5 times lower in comparison with AR state. This difference may be due to the difference of microstructure, but it may also reflect a higher trapping level in a quenched and tempered structure. Hydrogen penetrating into steel during SCC test could be more easily trapped in the QT state, inducing a better resistance to SSC of X52 steel in this state. Further investigation will be necessary to confirm this point.

#### 4. Conclusions

The obtained results can be summarised in the following way:

Resistance of API X52 and X60 steels depends strongly on their microstructure. This resistance can be increased considerably by quenching and tempering as in the case of HIC. The results show that SSC resistance cannot be derived from steel hardness or strength level only. If these findings are not respected, inappropriate materials can be chosen for wet  $\text{H}_2\text{S}$  service with all negative consequences. Hydrogen permeation tests showed a lower value of apparent hydrogen diffusion coefficient after quenching and tempering in comparison with as-received state, indicating thus, at least indirectly, a higher level of hydrogen trapping in a QT state.

#### Acknowledgements

*The experiments concerning SSC testing and electrochemical permeation tests were realised within a research plan MSM619890015 supported by the Ministry of Education of the Czech Republic. Structure analyses were supported by the grant project 106/04/0235 (Grant Agency of the Czech Republic).*

#### Literature

- [1] Brouwer R.C.: Int. J. Pres. Ves.& Piping, Vol. 56, 1993, p. 133.
- [2] Streisselberger A., Schwinn V.: In: Second Int. Conf. on Interaction of Steels with Hydrogen in Petroleum Industry Pressure Vessel and Pipeline Service, Vienna, Austria, 1994, p. 659.

- [3] Sojka J., Hyspecká L.: Acta Metallurgica Slovaca, Vol. 6, 2000, p. 327.
- [4] Kobayashi J. et al, in: Second Int. Conf. on Interaction of Steels with Hydrogen in Petroleum Industry Pressure Vessel and Pipeline Service, Vienna, Austria, 1994, p. 143.
- [5] NACE Standard MR 0175-95: Sulfide Stress Cracking Resistant Metallic Materials for Oilfield Equipment, NACE Int., Houston Texas, 1995.
- [6] Albarran J. L., Martinez L., Lopez H. F.: Corrosion Science, Vol. 41, 1999, p. 1037.
- [7] Carneiro R. A., Ratnapuli R. C., Treitas Cunha Lins V.: Materials Science and Engineering, A237, 2003, p. 104.
- [8] Devanathan M. A. V., Stachurski Z.: Proceedings of the Royal Society, London, A270, 1962, p. 90.
- [9] Manolatos P., Jerome M.: Electrochimica Acta, Vol. 41, 1996, p. 359.